Improvement of wear resistance of some cold working tool steels

Daniel Toboła [a], Witold Brostow [b,*], Kazimierz Czechowski [a], Piotr Rusek [a]

[a] Institute of Advanced Manufacturing Technology (IAMT), Wrocławska 37a, 30-011 Cracow, Poland
[b] Laboratory of Advanced Polymers & Optimized Materials (LAPOM), Department of Materials Science and Engineering and Department of Physics, University of North Texas, 3940 North Elm Street, Denton, TX 76207, USA

ARTICLE INFO

ABSTRACT

There are two basic options for improvement of surfaces of heat treated tool steels for cold working: mechanical treatment such as burnishing, or else chemical modification such as nitriding. The latter is affected not only by the nature of the chemical agent but also by diffusivity of that agent through the steel. We focus first on the number and order of operations performed on the steel surfaces: turned+burnished (T+B), turned+nitrided (T+B) and turned+burnished+nitrided (T+B+N). We have investigated two tool steels, Sverker 21 (AISI D2) and Vanadis 6. The former belongs to traditional steels, the latter is classified as advanced powder metallurgy (P/M) alloyed steel. We have performed pin-on-disc tribological experiments to determine abrasive friction and wear. Our evaluation of tribological properties of these two cold working steels enables an improvement of their manufacturing procedures leading to significant wear reduction. The improvement proposed is applicable not only to tool steels but also for instance to titanium alloys.

1. Introduction

Tools for metal forming (working) are essential for the production of metal parts in various industries. For example, the automotive industry in 2015 had a share of nearly 44% of metal parts on a global scale. Increasing car production in countries such as the US, China, Japan and Germany meant an increased demand for tools of these types [1].

Along with the increase in demand from the automotive industry, the global market for stamping / punching metals is growing at a steady pace. It is expected that the global market for metal forming will grow with an annual growth rate of 3% until 2019. With the increase in the use of metals in various fields such as transport, aerospace, automotive and precision industries (as shown in the example of the German market for metal forming in Fig. 1), the demand for tools for cold forming also increases [2,3].

Metal forming tools are made of tool steel obtained in the conventional metallurgical process, or else from powder metallurgy (P/M) and high speed steels (HSS).

According to Lind et al. [4] who discussed the case of blanking processes, there are three basic stages of tool wear. Abrasive wear is the first stage—facilitating the development of the adhesive wear (second stage). The final, fatigue wear is the third stage leading to ultimate destruction of the tool. One can control the speed of tool wear processes, among others, by changing the chemical composition of steel – increasing the content of alloying elements: tungsten, vanadium, and/or molybdenum.

Changing the method of steel production from conventional to powder metallurgy (P/M) allows to increase tools fatigue strength and obtain steels which have a uniform fine grain structure, characterized by higher hardness and toughness [5]. The use of a suitable combination of carbides in the structure of tool material also affects the properties [6]. Generation of compressive stresses in the tool surface layer improves the fatigue strength of high alloyed tool steels. Affecting the surface layer properties by manufacturing processes such as plastic deformation (eg. shot peening, roller and slide burnishing) results in generation of compressive stresses [7]. Burnishing may also be used to give good surface characteristics such as surface topography having oil pockets. According to Galda and coworkers [8] this technique is easy and results in formation of surfaces also in hard materials. Berkowski and Borowski [9] report good wear resistance for samples with the martensitic structures, burnished and nitrided at ≈ 400 °C).

Friction and adhesion of AISI 304L stainless steel against various commercial tool steels (four cold work steels and one high-speed steel) were tested by Määttä et al. [10]. They found that the composition of the tool steel does not have a marked effect on the friction between the tool and the workpiece. However, the surface roughness and topography of the tool have a significant influence.

Our area of interest is also improvement of wear resistance of cold working tool steels. A conventional D2 (AISI) steel, namely commercial grade Sverker 21 (from Uddeholm company) has been

* Corresponding author.
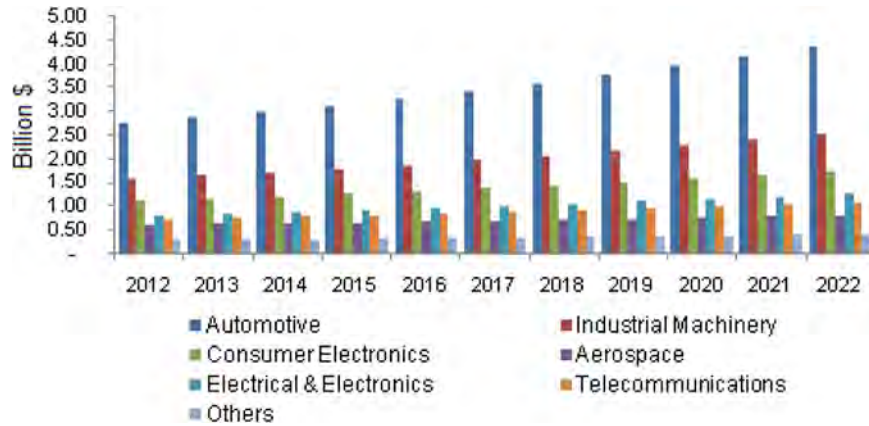   E-mail address: wkbrostow@gmail.com (W. Brostow).

Fig. 1. The market for metal forming in various industries in Germany in billions of US $ [3].

selected, together with Vanadis 6 steel. The former is a traditional steel, while Vanadis steels are modern powder metalurgy (P/M) steels containing very hard vanadium and molybdenum carbides which replace softer chromium carbides [11,12]. Introduction of very hard structural components in the cold working tools like punches and dies is known to increase the resistance to the abrasive action of shaped materials. However, hardness it is not the only criterion reflecting the wear resistance of tool materials. Steels of comparable hardness will wear in variable manner when type, size or distribution of carbides are different [6]. Apart from advanced tool materials with controlled structures there are more possibilities of abrasive resistance improvements of martensitic steels achieved by joined manufacturing technology which combines operations of machining, burnishing and nitriding [13]. Shot peening technology [14–16] seems to be widely used in automotive and aircraft industry. Prevey [17] showed, however, that static burnishing (such as roller and slide burnishing) ensures better surface properties than dynamic burnishing or shot peening. One has a control of the depth of plastic deformation, whereas shot peening generates a large density of dislocations in the surface layer resulting from the high stresses; in turn, this causes an unstable state of internal stresses. Wide scatter of results obtained with this technique is seen. Another possibility for extending tool lives (high abrasive wear resistance) provide e.g. hard PVD nitride of carbides coating [18–21] self-mating layers [22], laser cladding [23], nitrocarburizing [24], ion nitriding [25] and combination of deep-cryogenic treatment with plasma nitriding [26].

2. Experimental procedure

2.1. Materials and procedure

The nominal chemical compositions of the two grades are presented in Table 1. Samples from both steels were cut and heat treated as indicated in Table 2. The final macrohardness of both tool steels after the heat treatment (HT) was $\approx$ 60 HRC.

After the heat treatment, the specimens were subjected to different surface treatment defined in Fig. 2.

Turning process applying PCBN (*polycrystalline cubic boron nitride*) cutting inserts with commercial names NP-SNGA 120412GS2 MB730 was performed by using a constant feed $f=0.17$ mm/rev. and the cutting depth $a_p=0.1$ mm. Cutting speeds were different: $v_c=100$ m/min for Sverker 21 and $v_c=150$ m/min for Vanadis 6; the objective here was achieving for both steels similar surface roughness Ra values (averaged from 6 measurements) before burnishing, namely in the range from 0.72 to 0.82 μm.

Slide diamond burnishing of our tool steels in the quenched

Table 1
Chemical compositions of the steels (wt%).

Steel	C	Si	Mn	Cr	Mo	V	
Sverker 21	1.55	0.3	0.4	11.8	0.8	0.8	C/M steel
Vanadis 6	2.1	1.0	0.4	6.8	1.5	5.4	P/M steel

C/M steel made by a conventional way, P/M steel made by powder metallurgy.

Table 2
Heat treatment parameters for Sverker 21 and Vanadis 6 tool steels.

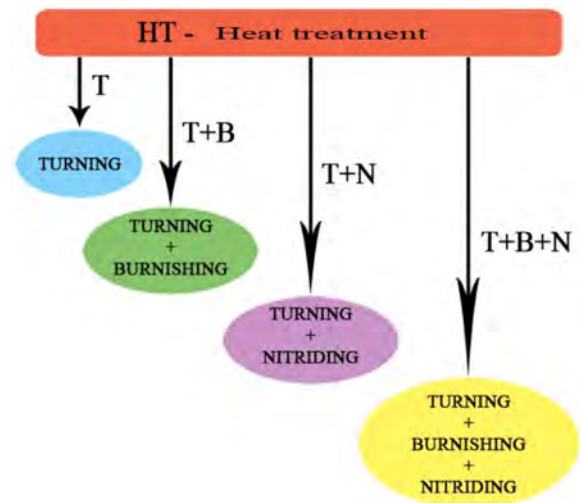|	Sverker 21	Vanadis 6
Austenitizing First tempering Second tempering	1035–1040 °C, 4 min 30 s 530 °C, 2 h 520 °C, 2 h	1070 °C, 4 min 30 s 550 °C, 2 h 520 °C, 2 h

Fig. 2. Scheme of different types of surface treatments used during the studies.

Table 3
Parameters applied in the slide diamond burnishing process with the tool radius R=1.5 mm.

Parameters	Tool steel	
	Sverker 21	Vanadis 6
Speed v, m/min	40	
Feed f, mm/rev.	0.02	
Force F, N	180	160
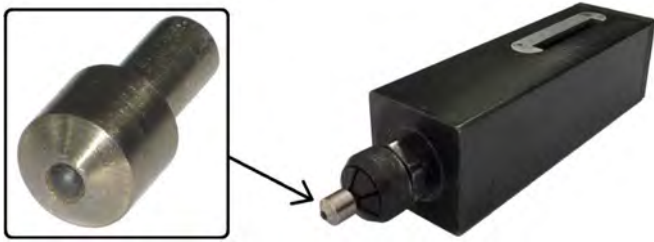
Fig. 3. Diamond burnisher (spherical cups) with tool holder and working parts.

Table 4
Type of surface treatment and resulting roughness.

Tool Steel	Surface treatment	Sample code	Mean Ra roughness, μm
Sverker 21	HT+T	S.1	0.8
	HT+T+B	S.2	0.24
	HT+T+N	S.3	0.72
	HT+T+B+N	S.4	0.23
Vanadis 6	HT+T	V.1	0.78
	HT+T+B	V.2	0.24
	HT+T+N	V.3	0.78
	HT+T+B+N	V.4	0.27

state was carried out using diamond tools - with parameters listed in Table 3. These tools (Fig. 3) are designed and currently produced at our IAMT, with the tips in the shape of spherical caps. High pressure-high temperature (HT-HP) Bridgman type apparatus was used to obtain diamond composites with ceramic bonding phase, namely Ti_3SiC_2.

Compacts were sintered at the pressure of 8.0 ± 0.2 GPa and at 1800 ± 50 °C for 30 s. Subsequently, their spherical shapes were formed by electrical discharge machining (EDM) [27,28].

After turning or turning+burnishing processes, selected surfaces were immediately nitrided by gas nitriding, under following conditions: first stage at 520 °C/5 h and second stage at 535 °C/ 20 h.

2.2. Friction determination and wear testing

The abrasive wear resistance was evaluated by pin-on-disc method (Fig. 4a), using a CETR UMT- 2MT universal mechanical tester from Campbell City, CA, USA. Beyond the determination of dynamic friction, this test allows determination of abrasive wear—the most dominant wear mechanism in all cold forming operations according to Podgornik and Leskovšek [29]. Considering the typical wear of tool steels in cold forming, we have used Al_2O_3 pins.

The loading mechanism applies a controlled load F_n to the pin holder and the friction force is measured continuously during the test using an extensometer. For each test, a new pin was used or the pin was rotated so that a new surface was in contact with the disc. The pin and discs were washed in ethyl alcohol and dried. The size of the disc-shaped samples was ≈ 30 mm diameter and ≈ 20 mm in height with the surfaces flatness and parallelism within 0.02 mm. The following test conditions were applied: pin diameter $=3.2$ mm, the applied load $=6.0$ N, the sliding speed

$=0.1$ m/s, diameter of the sliding circle $=8$ mm, sliding distance $=2000$ m, calculated duration of the test 20,000 s. For each type of surface treatments three tests were carried out at room temperature (25 ± 2 °C) without lubricant, under maximum Hertzian contact pressure 2180 MPa and 2150 MPa, respectively, for Vanadis 6 and Sverker 21 steels. The test conditions were defined so that the contact pressure did not exceed the yield strength of the tested steels; this way we have eliminated the plastic deformation—the other type of damage mechanism in cold working processes. Given four types of surface treatments used, the chosen pin-on-disc test parameters allow good assessment of the impact of those treatments on abrasive wear.

After completing the tests according to the ISO 20808:2004 E standard, the cross-sectional profiles of the wear tracks at four locations at intervals of 90° were measured using a contact stylus profilometer TOPO 01. Then the average cross-sectional areas of the wear tracks were calculated; see Fig. 4b. The volume of material removed was calculated as a product of the cross-sectional area of the wear track and their circumference. That is

$$W_s = \frac{V}{F_n \oplus L} \tag{1}$$

where W_s=specific wear rate, V=volume of the removed material, while L=sliding distance.

The roughness of the tested surface before wear test was dependent on the type of surface treatment applied; see Table 4.

2.3. Microscopic examinations

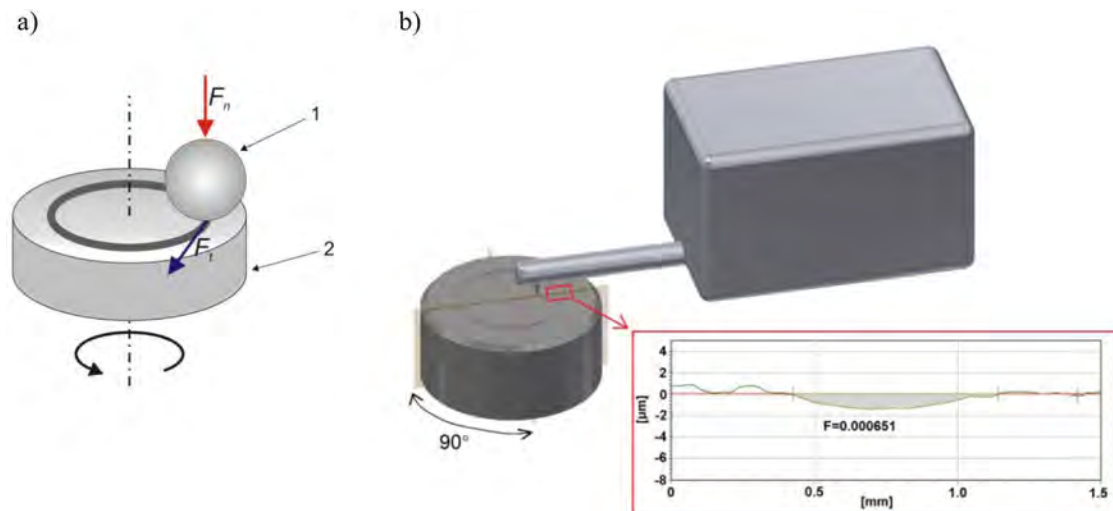Metallographic structures were observed with an optical Carl

Fig. 4. Schemes of: a) pin-on-disc tests 1=Al_2O_3 ball; 2=sample (disc), b) cross-sectional profile measurement of the wear track.

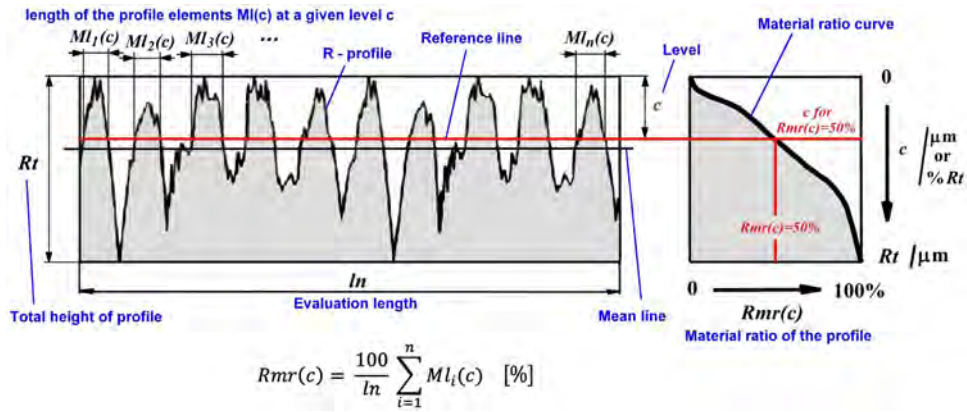$$Rmr(c) = \frac{100}{ln}\sum_{i=1}^{n} Ml_i(c) \quad [\%]$$

Fig. 5. Rmr(c)=material ratio of the profile according to the ISO 4287 standard [30].
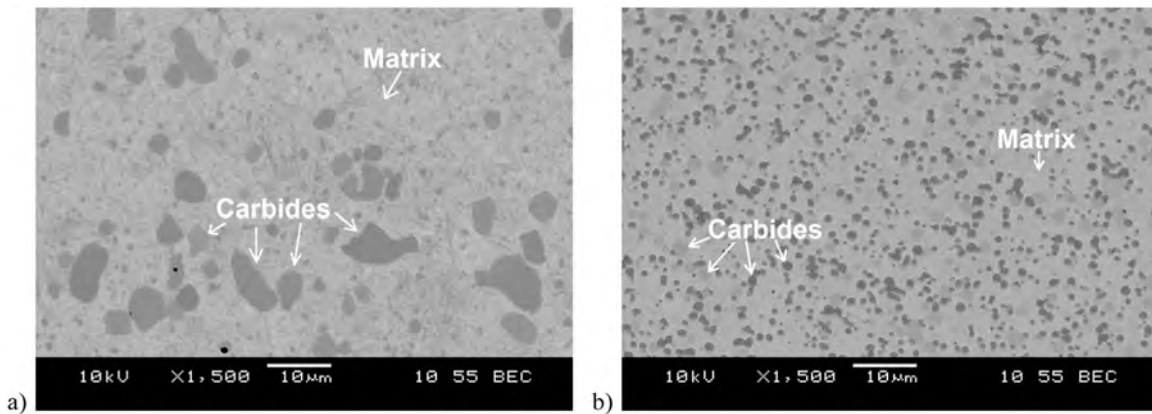

Fig. 6. Microstructure of two studied steels: a) Sverker 21, b) Vanadis 6.
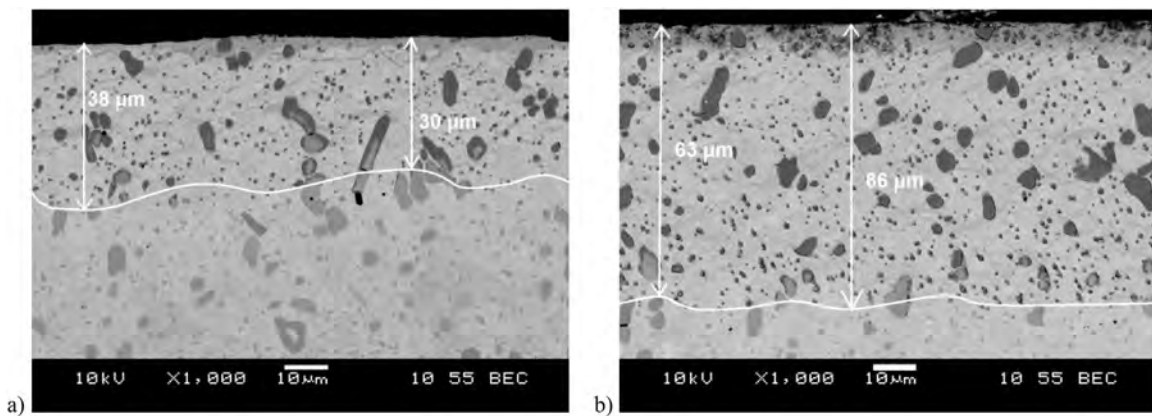

Fig. 7. Cross-sectional SEM micrograph of Sverker 21 steel surface layer after: a) turning+nitriding, b) turning+burnishing+nitriding.

Zeiss Axiovert 100 A microscope and a scanning electron microscope (JEOL type JSM-6460LV) equipped with an INCA EDS (energy dispersive X-ray spectrometer).

2.4. Hardness measurements

Vickers microhardness $h_{Vickers}$ was determined using a FM 7 tester from Future Tech. Corp., Japan. Microindentations were made using a 10.0 g load. On each specimen 3 measurements were performed at various distances below the surface in order to obtain representative average hardness value.

2.5. GDOES analysis

The distribution of the concentrations of N and C along the thickness of the surface layer was determined using the GDOES (glow discharge optical emission spectrometry) method, employing a GDS 850A spectrometer made by LECO. The discharge parameters were: cathode voltage =700 V, ion current =25 mA; a 4 mm diameter anode were used.

2.6. Surface roughness analysis

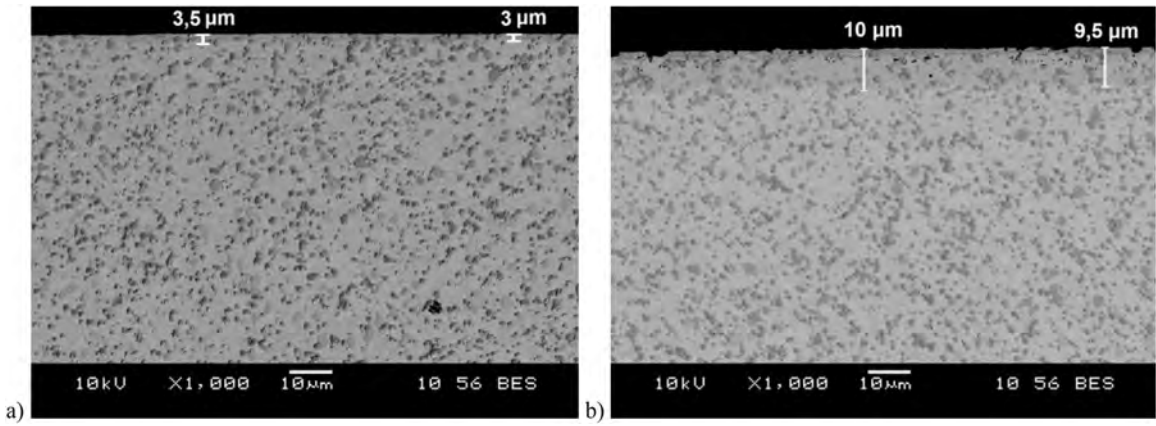The surface roughness parameter Ra was measured with the

Fig. 8. Cross-sectional SEM micrograph of Vanadis 6 steel surface layer after: a) turning+nitriding, b) turning+burnishing+nitriding.
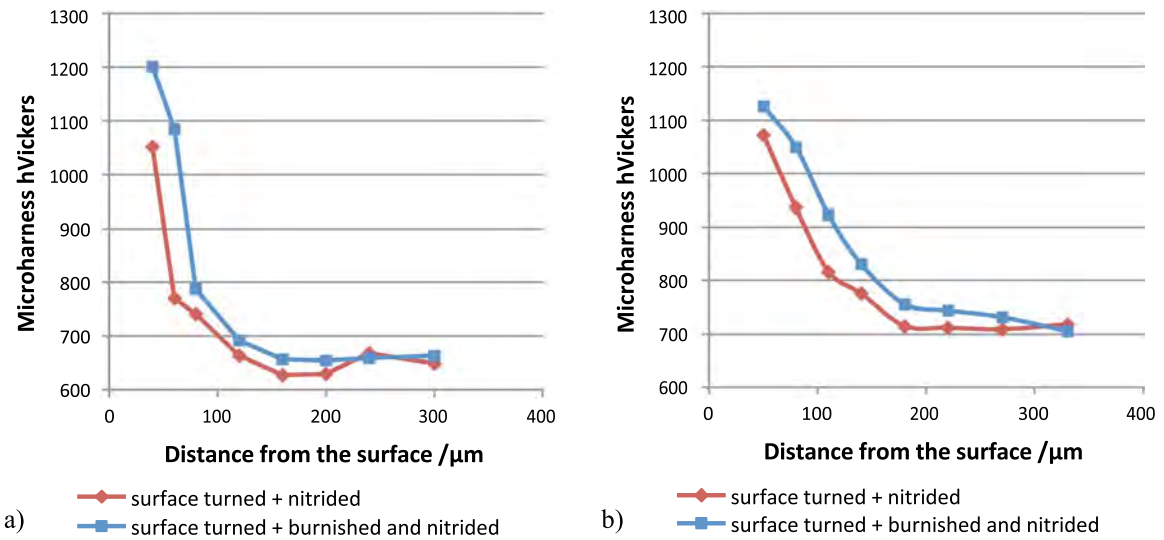

Fig. 9. Microhardness of Sverker 21 (a) and Vanadis 6 (b) specimens after turning, slide diamond burnishing and nitriding.
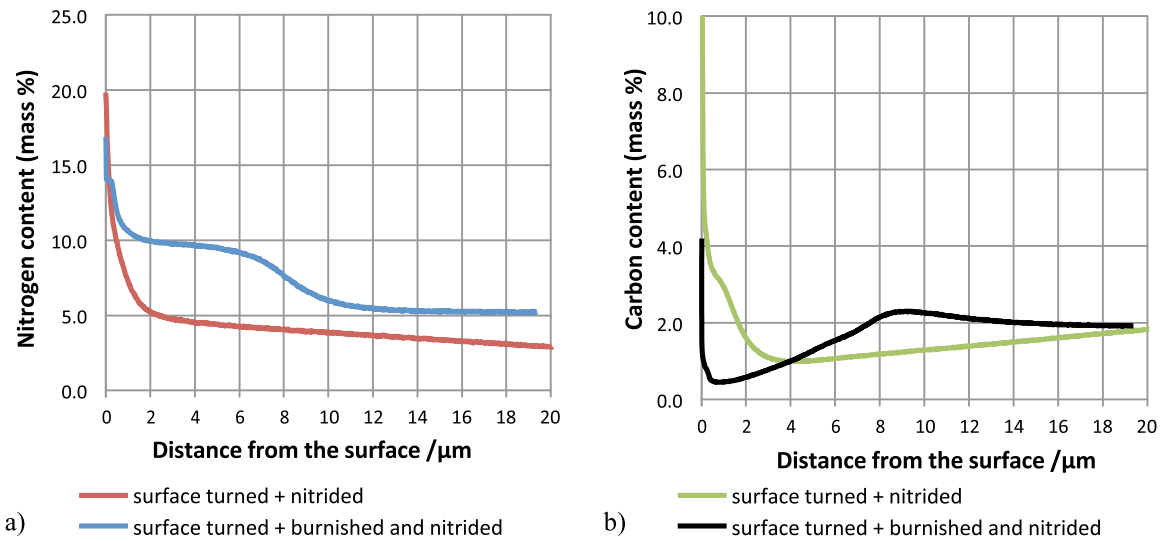

Fig. 10. Profiles of a) nitrogen and b) carbon content for Sverker 21 steel surface layers after turning+nitriding or turning+burnishing+nitriding.

Hommel Tester T1000E profilometer and with a laboratory TOPO 01 profilometer produced at IAMT. We have calculated the index of roughness change as

$$K_{Ra} = \frac{Ra'}{Ra} \qquad (2)$$

where Ra' is the value before burnishing and Ra afterwards; the same parameters have been used by Janczewski et al. in work on polyethylene [30].

A particularly important parameter influencing directly the tribological properties is the material ratio of the profile,
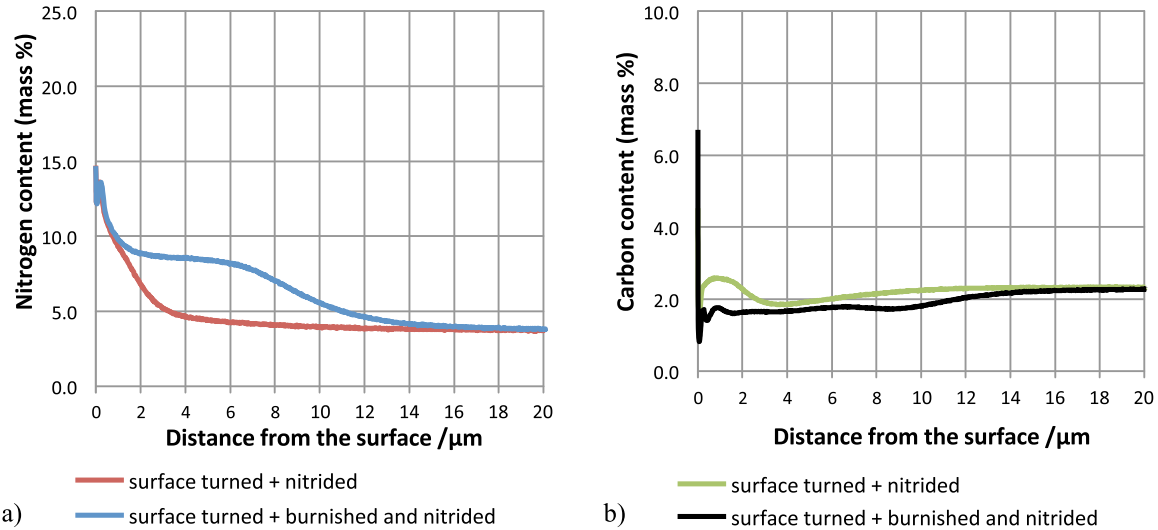
Fig. 11. Profiles of a) nitrogen and b) carbon content for steel Vanadis 6 surface layers after turning+nitriding or turning+burnishing+nitriding.

Table 5
Surface geometry (SG) parameters; for samples codes see Table 4.

Sample Code	Burnishing Force F N	Feed f mm/rev	SG parameters after turning					SG parameters after burnishing					K_{Ra}
			Ra' μm	Rz' μm	Rp' μm	Rt' μm	c', % Rt for Rmr'(c)=50	Ra % μm	Rz μm	Rp μm	Rt μm	c, % Rt for Rmr(c)=50%	
V.1	Turning		0.77	3.19	1.99	3.35	67	–	–	–	–	–	–
V.2	160	0.02	0.80	3.81	2.44	4.34	62	0.24	1.60	0.95	2.00	47	3.32
V.3	Turning		0.78	3.32	2.17	3.53	69	–	–	–	–	–	–
V.4	160	0.02	0.79	3.68	2.34	4.09	64	0.27	1.73	1.23	2.29	53	2.96

Remarks:
Lt=4.8 mm (*traverse length*); Ra=*arithmetical mean deviation of the assessed profile*; Rz=*the average maximum profile height of the ten greatest peak-to-valley separations in the evaluation area*; Rp=*maximum profile peak height (is the distances from the mean line/surface to the highest point in the evaluation length/area)*; Rt=*total height of profile*; Rmr (c)=*material ratio of the profile*; c, % Rt for Rmr(c)=50%=*the value of the reference level 'c' for Rmr(c)=50%*;
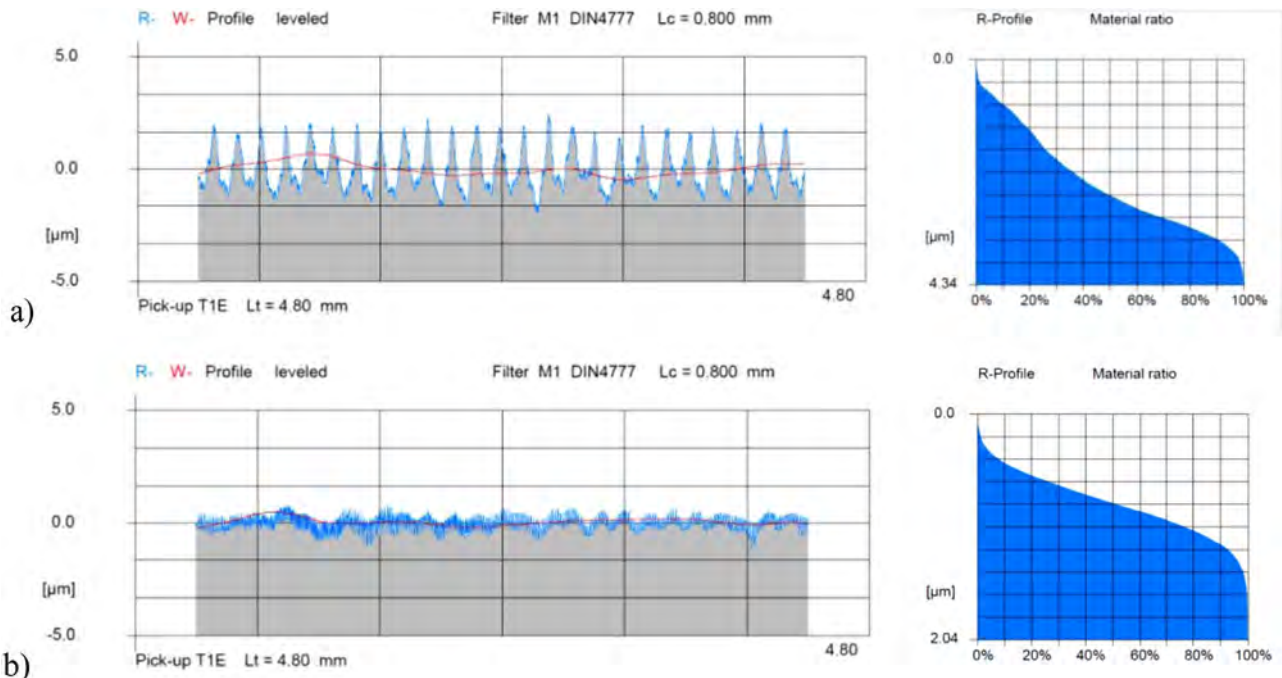Surface roughness parameters determined according to ISO 4287.

Fig. 12. Examples of the profilographs and the material ratio of the profile for the Vandis 6 specimens surface after: a) turning, b) turning–burnishing. R is the 2D roughness profile, W is the waviness profile, Lc is the cut-off wavelength filter.
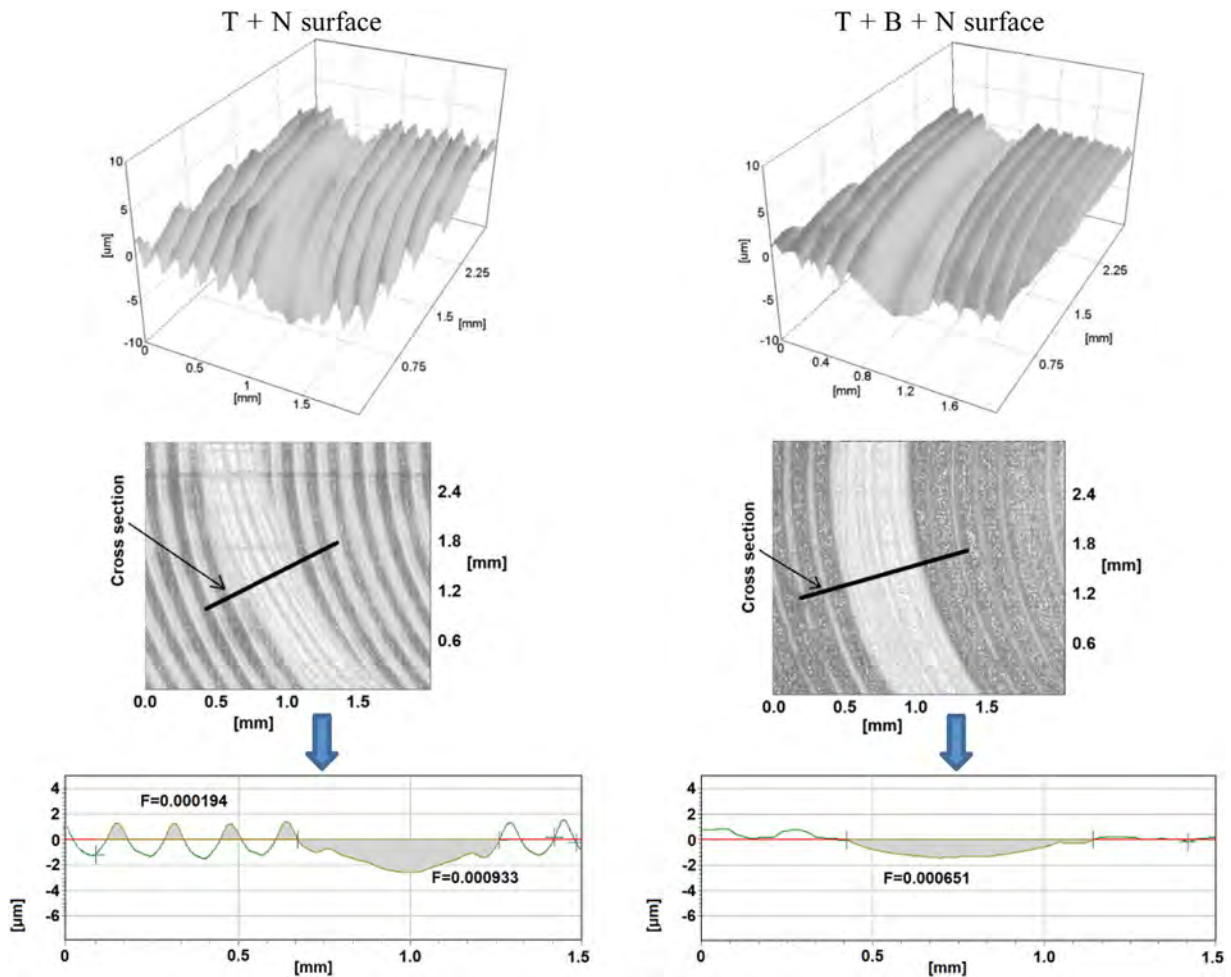
Fig. 13. Wear traces after the pin-on-disc tribological test on Vanadis 6 steel specimens subjected to various surface treatments; shown in 3-D (top), contour maps (middle) and 2-D (bottom).
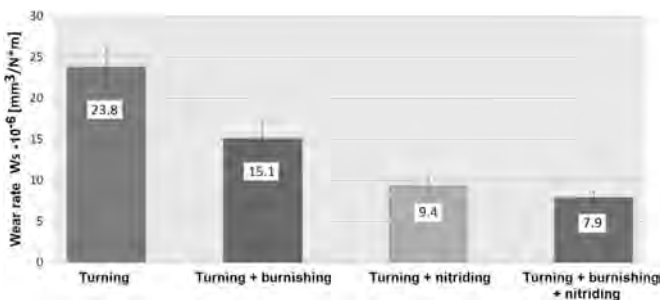

Fig. 14. Wear rates obtained in pin-on-disc testing of Sverker 21 steel after various surface treatments.
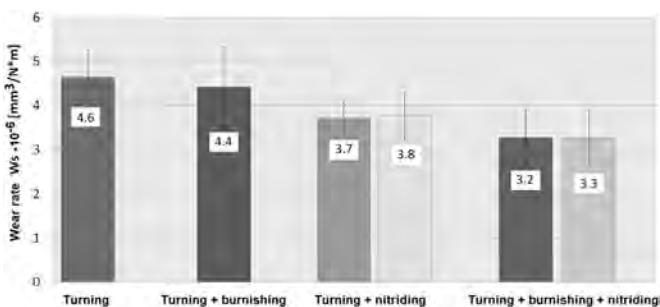

Fig. 15. Wear rates obtained in pin-on-disc testing of Vanadis 6 steel after various surface treatments.

determined as illustrated in Fig. 5 and discussed earlier for polyethylene in [30].

3. Microstructural studies

In Fig. 6 we show microstructures of our steels after heat treatment: Sverker 21 on the left (a) and Vanadis 6 on the right (b). In both cases we see carbide particles within a fine tempered martensite matrix. Differences are seen in the size and uniformity distribution of carbides.

Figs. 7 and 8 show the cross-sectional microstructure of our steels subjected to various surface treatment processes. Fig. 7 already appeared in [31] but is included here for comparison.

The total thickness of specific compound zones in the turned and nitrided Sverker 21 steel sample reaches $\approx 40\,\mu m$ (Fig. 7a). In the case of the specimen which additionally had been slide burnished by a diamond composite tool before nitriding, the thickness of the compound zones is $\approx 65\,\mu m$ (Fig. 7b).

For the Vanadis 6 steel, for surfaces only turned and nitrided, the thickness of the compound zone reaches locally $\approx 3.5\,\mu m$ (Fig. 8a); however it reaches $\approx 10\,\mu m$ (Fig. 8b) after the combined process. In the process without burnishing, the thickness variations are $\approx 0.5\,\mu m$; for processing including burnishing, these variations also do not exceed $\approx 0.5\,\mu m$.
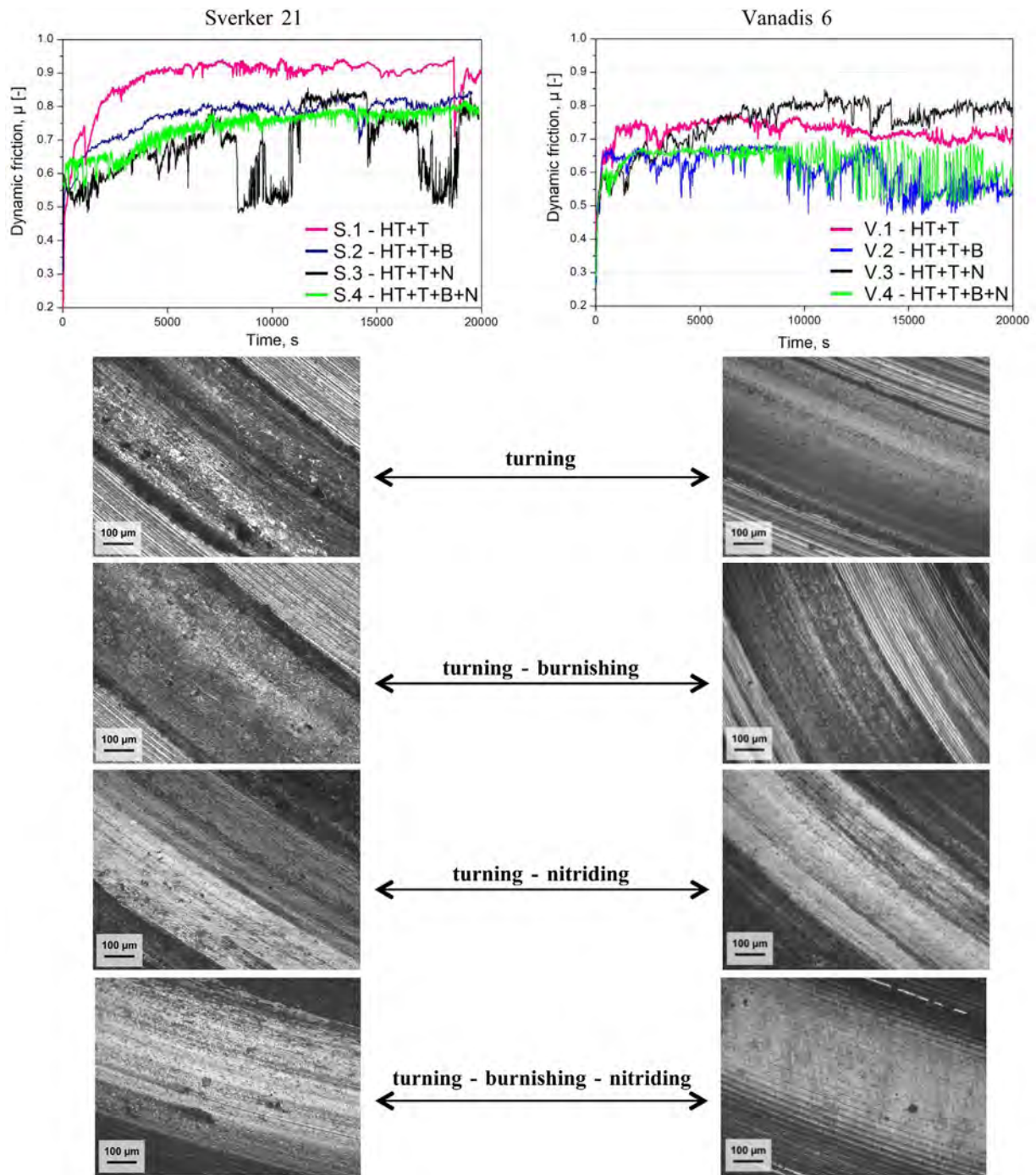
Fig. 16. Dynamic friction μ, determined in pin-on-disc tests, for our steels after various surface treatments. Lower part: micrographs of Sverker 21 (left) and Vanadis 6 (right) steel surfaces.

4. Hardness

We have determined the Vickers microhardness $h_{Vickers}$, a quantity we have used before to characterize other types of materials and coatings [32]. For nitrogenized surfaces of our steels we observe a significant increment of the microhardness (Fig. 9). The increment amounts to 10% for burnished surfaces as compared to surfaces nitrided only. Results of the hardness distribution for Sverker 21 steel have been reported in [31] but are included here for comparison; hardening of the surface which had been turned and burnished before nitriding takes place to a depth reaching

$\approx 80\ \mu m$. Differences amount to between 4 and 44% for the surfaces nitrided or otherwise.

5. GDOES analysis

Figs. 10 and 11 shows the results of profile analysis for carbon and nitrogen obtained by GDOES for our steels subjected to various combinations of surface treatments. Results for the layer depth of 20 μm below the surface are reported. The use of three stage process (turning-burnishing-nitriding) leads as expected to increased nitrogen
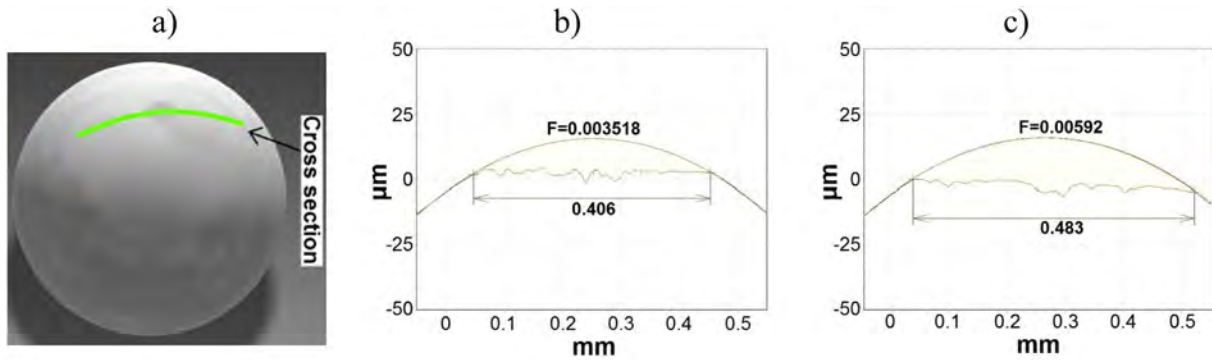
Fig. 17. Examples of 2-D transverse profiles of Al₂O₃ pins (a) in the wear trace areas pin-on-disc testing of Sverker 21 (b) and Vanadis 6 (c) steels.

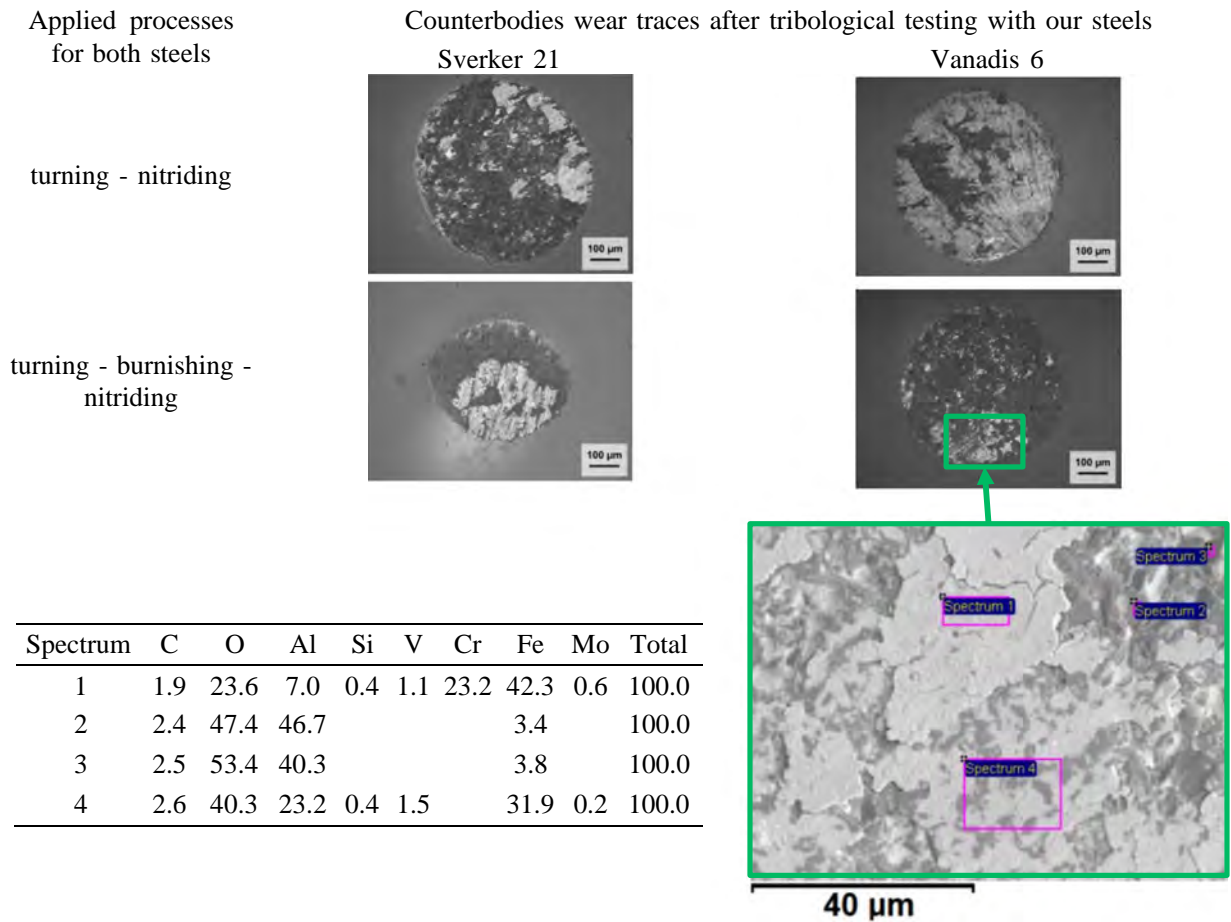| Spectrum	C	O	Al	Si	V	Cr	Fe	Mo	Total
1	1.9	23.6	7.0	0.4	1.1	23.2	42.3	0.6	100.0
2	2.4	47.4	46.7				3.4		100.0
3	2.5	53.4	40.3				3.8		100.0
4	2.6	40.3	23.2	0.4	1.5		31.9	0.2	100.0

Fig. 18. Examples of wear traces on Al₂O₃ pins after tribological testing of steels, together with the chemical analysis of microareas of the chosen trace.

content. As for the surface layer carbon content, a reduction is observed. It is apparently caused by carbon diffusion towards the core [33,34].

6. Effect of surface treatment processes on the surface roughness

Values of surface roughness parameters (Ra, Rz, Rp, etc.) including K_{Ra} index defined by Eq. (2) after the surface treatment processes for steels are listed in Table 5. The results for Sverker 21 steel were already included in an earlier paper [31].

We see in Table 5 that slide burnishing favorably affects the SG properties. Ra and other parameters are much lower after burnishing.

We provide the roughness profiles in Fig. 12 for Vanadis 6 steel, while those for Sverker 21 were presented in an earlier paper [31]. We see how the height of the profile decreases after burnishing. There is reduction, by more than a factor of two, of the parameter c%, namely Rt for Rmr′(c)=50%; we see also a concurrent increase in the material ratio, what substantially increases the area of tool/workpiece contact.

7. Effect of the combined processes on abrasive wear

According to the classical work of Archard [35] who formulated one of the most widely used wear models, chemical, physical and mechanical effects have all to be taken into account when analyzing wear. The wear rate can be considered as a stochastic

process. Contributions to wear can have different magnitudes. Thus, for a ceramic and steel, the former has a propensity for brittle fracture while the latter for adhesive wear. This difference in mechanical properties is crucial for the resulting wear resistance.

Apparently there is migration of material from the surface with a lower hardness towards the surface with a higher hardness (for the analyzed case from the steel sample surface to the surface of ceramic ball). Then sliding friction between the same materials is seen, accompanied by strong adhesion of surfaces, visible in the form of matt wear signs at the surfaces.

Fig. 13 shows an example of the profile of the wear traces, in 2-D and 3-D, for the surfaces of Vanadis 6 tool steel, after 2 processing variants.

We now consider the wear values for the Sverker 21 steel, as shown in Fig. 14. Compared with the one-stage turning operation, both burnishing and nitriding after turning produce wear reduction. However, the effect is significantly larger for nitriding. Best of all is the three stage process; compared to turning alone, the reduction of wear amounts to 67%.

The Vanadis 6 steel has much higher wear resistance to begin with, see Fig. 15. After turning only, the wear amounts to $4.6 \cdot 10^{-6}$ [mm^3/N m]. As expected, burnishing or nitriding provide wear reductions. The tree-stage process provides a reduction amounting to 30%.

We have also considered the effects of time on wear values. For this purpose, we have studied turned and nitrided as well as three-stage treated Vanadis 6 steel samples *six months* after the surface treatments. The results are shown as lightly shaded rectangles in Fig. 15. Virtually no effect of time on wear values is seen.

8. Effects of the combined processes on dynamic friction

Fig. 16 shows the dynamic friction results after various surface treatments for both steels. For Sverker 21 steel, during turning the dynamic friction increases with sliding time up to about 60 min; then it reaches a practically constant value of about 0.9. A similar trend can be observed after burnishing, but then the asymptotic value is approximately 0.8. A different trend is observed after turning and nitriding. Two dangerous stages occurred (after about 2 h and 4.5 h), which normally correspond to surface fatigue scale off. A similar phenomenon has been observed by Staia et al. [36]. Sequential processing: turning-burnishing-nitriding resulted in the asymptotic value of the dynamic friction of ≈ 0.75. For the Vanadis 6 steel, for turned surface, the dynamic friction increases for the first 20 min.; then it reaches a value of 0.75, subsequently only small variations were recorded. For the surface burnished before nitriding, the value is smaller, below 0.65; for turning-nitriding, friction reaches initially 0.6, but then quickly increases to 0.8. For the surface burnished before nitriding, dynamic friction is 0.65 at about 2.5 h., and this is followed by characteristic fluctuations in the range 0.5–0.7.

In the lower part of Fig. 16 we show optical micrographs of surfaces of both steels. Wear traces on sample surfaces were changing with application of subsequent strengthening technology. Matt surfaces are more common for turning and turning-burnishing technology. For strengthened surfaces, burnished and subsequently nitrided, the wear traces are mostly bright, without matt areas. This effect occurs for both steels. Transfer of the sample material (less hardened steel) on the counterbody pin occurs even for Vanadis 6 steel (compare with Fig. 18). Micro adhesive tacks welding appear as matt areas on wear tracks along the sample surfaces.

In addition to optical observations and chemical analyses of the microareas of wear traces of Al$_2$O$_3$ pins, their shape was measured

before and after pin-on-disc testing. Fig. 17 shows that for Vanadis 6 there is a nearly twice larger wear as for Sverker 21. One of the possible reasons for this difference can be the type of carbides in the two steels – as reflected in different hardness values. According to Nurthen and coworkers [12], due to much higher vanadium content in Vanadis 6 steel relative to Sverker 21, more carbides rich in vanadium appear in the former, imparting much higher hardness than chromium carbides dominant in Sverker 21. We recall that cermets, or combinations of carbides with tool steels, are usable at higher temperatures than such steels without carbides [37].

Fig. 18 shows optical micrographs of wear traces of Al$_2$O$_3$ counterbodies. We also provide a table of chemical compositions of the wear trace microareas for chosen processing variants. The results indicate a material transfer from the steels to the surfaces of the counterbodies.

9. A survey of results

Apparently in our hybrid three-stage process there is some synergy between the consecutive stages. Leaving out the burnishing step may result in a reduction of end-use properties of tools. The significant effects of applying the T+B+N process to the cheaper Sverker 21 steel, increases the possibility of the wider use of the process, in turn limiting the use of the more expensive tool steels. Needless to say, this would improve the economic situation of a company for which tool costs are a significant part of its production costs.

The additional incorporation of slide burnishing results in the geometric surface structure becoming less resistant to friction and larger material ratio, which can favorably influence the cooperation of contacting areas so produced.

Surface geometry of the cold working tool with a low roughness and good bearing area after hybrid (HT+B+N) technology imposed mostly by two operations: hard turning and burnishing combination needs only light manual polishing before its industrial application.

For both our steels, nitriding gives better results when preceded by burnishing. The upper surface layer allows then easier and deeper reception of nitrogen. Homogeneity defined as a lack of thickness variation of nitrided layer is much better for HT+B+N technology for both our steels than for any alternative manufacturing procedures. Consequences for durability of the cold working tools are evident.

The fact that our procedure is applicable to both conventional steels (our Sverker 21) and advanced powder metallurgy alloyed steels (our Vanadis 6) is an advantage. Consider now the system reliability in mass series production. Application of our three-stage technology would reduce the amount of changeover of tools, or else reduce the time intervals at which the changeover becomes necessary.

References

[1] Global Metal Forming Machine Tools Market 2016–2020, December 2015. ⟨http://www.researchandmarkets.com/reports/3534920/global-metal-forming-machine-tools-market-2016⟩.

[2] Metal Stamping Market to 2019 Demand from Automotive Industry Drives the Growth, ⟨http://www.barchart.com/headlines/story/4316190/metal-stamping-market-to-2019⟩.

[3] Metal Stamping Market Analysis By Technology (Blanking, Embossing, Bending, Coining, Flanging), By Application (Automotive, Industrial Machinery, Consumer Electronics, Aerospace, Electrical & Electronics, Telecommunications,) and Segment Forecasts to 2022; ⟨http://www.grandviewresearch.com/industry-analysis/metal-stamping-market⟩.

[4] L. Lind, P. Peetsalu, P. Podra, E. Adoberg, R. Veinthal, P. Kulu, Description of punch wear mechanism in Turing fine banking process, in: Proceedings of 7th International DAAAM Baltic Conference "Industrial Engineering", Tallinn, 2010.

[5] A. Kolja, M. Marion, Improvement of surface integrity of cold forming tools by adaption of tool making process, Prod. Eng. Res Dev. 8 (2014) 131–141.

[6] L. Bourithis, G.D. Papadimitriou, J. Sideris, Comparison of wear properties of tool steels AISI D2 and O1 with the same hardness, Tribol. Int. 39 (2006) 479–489.

[7] V. Chomienne, F. Valiorgue, J. Rech, C. Verdu, Influence of ball burnishing on residual stress profile of a 15-5PH stainless steel, CIRP J. Manuf. Sci. Technol. 13 (2016) 90–96.

[8] L. Galda, W. Koszela, P. Pawlus, Surface geometry of slide bearings after percussive burnishing, Tribol. Int. 40 (2007) 1516–1525.

[9] L. Berkowski, J. Borowski, The influence of structure on the results of the nitriding of ledeburitic chromium steels. Part VIII. Investigation of utilization properties of tool materials, Metal. Form. (Obróbka Plast. Met.) 4 (2009) 3–16.

[10] A. Määttä, P. Vuoristo, T. Mäntylä, Friction and adhesion of stainless steel strip against tool steels in unlubricated sliding with high contact load, Tribol. Int. 34 (2001) 779–786.

[11] S. Wilmes, G. Kientopf, Carbide dissolution rate and carbide contents in usual high alloyed tool steels at austenitizing temperatures between 900 ºC and 1250 ºC, in: Proceedings of the 6th International Tooling Conference, Karlstad, 2002, pp. 533–547.

[12] P. Nurthen, O. Bergman, I. Hauer, Carbide design in wear resistant powder materials, in: Proceedings of the PM 2008 World Congress in Washington, DC, 2008, pp. 1–16.

[13] R.M. Muñoz Riofano, L.C. Castelitti, L.C.F. Canale, G.E. Totten, Improved wear resistance of P/M tool steel alloy with different vanadium contents after ion nitriding, Wear 265 (2008) 57–64.

[14] B. Hashemi, M. Rezaee Yazdi, V. Azar, The wear and corrosion resistance of shot peened-nitrided 316L austenitic stainless steel, Mater. Des. 32 (2011) 3287–3292.

[15] M. Ariati, R. Aldila, Application of shot peening and shot blasting to increase hardness and depth of nitride hardened layer to the modified H13 steel as die casting die materials, Adv. Mater. Res. 789 (2013) 313–319.

[16] L. Alzati, U. Engström, B. Rivolta, A. Tavasci , Wear resistance of gas nitrided astaloy CrL^{TM} sintered steel, in: Proceedings of the PM 2008 World Congress in Washington, DC, 2008, pp. 201–208.

[17] P.S. Prevéy, N. Jayaraman, J. Cammett, Overview of low plasticity burnishing for mitigation of fatigue damage mechanisms, in: V. Schulze, A. Niku-Lari (Eds.), Proc. 9th Intl. Conf. on Shot Peening (ICSP9), Paris, IITT International, 2005, pp. 267–72.

[18] F. Sergejev, P. Peetsalu, A. Sivitski, M. Saarna, E. Adoberg, Surface fatigue and wear of PVD coated punches during fine blanking operation, Eng. Fail Anal. 18 (2011) 1689–1697.

[19] W. Tillmann, E. Vogli, S. Momeni, Mechanical and tribological properties of Ti/TiAlN duplex coatings on high and low alloy tool steels, Vacuum 84 (2010) 387–392.

[20] B. Podgornik, B. Zajec, N. Bay, J. Vižintin, Application of hard coatings for blanking and piercing tools, Wear 270 (2011) 850–856.

[21] B. Podgornik, M. Sedlaček, M. Čekada, S. Jacobson, B. Zajec, Impact of fracture toughness on surface properties of PVD coated cold work tool steel, Surf. Coat. Technol. 277 (2015) 144–150.

[22] S. Hanke, M. Beyer, J.F. Santos, A. Fischer, Friction surfacing of a cold work tool steel – microstructure and sliding wear behaviour, Wear 308 (2013) 180–185.

[23] M. Pleterski, T. Muhič, B. Podgornik, J. Tušek, Blanking punch life improvement by laser cladding, Eng. Fail Anal. 18 (2011) 1527–1537.

[24] C.-M. Karamboiki, A. Mourlas, P. Psyllaki, J. Sideris, Influence of microstructure on the sliding wear behavior of nitrocarburized tool steels, Wear 303 (2013) 560–568.

[25] K.T. Cho, Y.-K. Lee, W.B. Lee, Wear behavior of AISI D2 steel by enhanced ion nitriding with atomic attrition, Tribol. Int. 87 (2015) 82–90.

[26] B. Podgornik, F. Majdic, V. Leskovsek, J. Vizintin, Improving tribological properties of tool steels through combination of deep-cryogenic treatment and plasma nitriding, Wear 288 (2012) 88–93.

[27] L. Jaworska, L. Stobierski, A. Twardowska, D. Królicka, Preparation of materials based on Ti–Si–C systems using high temperature–high pressure method, J. Mater. Process. Technol. 162–163 (2005) 184–189.

[28] L. Jaworska, M. Szutkowska, J. Morgiel, L. Stobierski, J. Lis, Ti$_3$SiC$_2$ as a bonding phase in diamond composites, J Mater. Sci. Lett. 20 (2001) 1783–1786.

[29] B. Podgornik, V. Leskovšek, Wear mechanisms and surface engineering of forming tools, Mater. Technol. 49 (2015) 313–324.

[30] Ł. Janczewski, D. Toboła, W. Brostow, K. Czechowski, H.E. Hagg Lobland, M. Kot, K. Zagórski, Effects of ball burnishing on surface properties of low density polyethylene, Tribol. Int. 93 (2016) 36–42.

[31] D. Toboła, W. Brostow, K. Czechowski, P. Rusek, I. Wronska, Structure and properties of burnished and nitride AISI D2 tool steel, Mater. Sci. Medžiagotyra 21 (2015) 511–516.

[32] W. Brostow, K. Czechowski, W. Polowski, P. Rusek, D. Toboła, I. Wronska, Slide diamond burnishing of tool steels with adhesive coatings and diffusion layers, Mater. Res. Innov. 17 (2013) 269–277.

[33] I. Calliari, M. Dabalà, E. Ramous, M. Zanesco, E. Gianotti, Microstructure of a nitrided steel previously decarburized, J. Mater. Eng. Perform. 15 (2006) 693–698.

[34] M.A. Passin, M.D. Tier, T.R. Strohaecker, A. Bloyce, Y. Sun, T. Bell, The effect of plasma nitriding process parameters on the wear characteristics of AISI M2 tool steel, Tribol. Lett. 8 (2000) 223–228.

[35] J.F. Archard, Contact and rubbing of flat surfaces, J. Appl. Phys. 24 (1953) 981–988.

[36] M.H. Staia, Y. Pérez-Delgado, C. Sanchez, A. Castro, E. Le Bourhis, E.S. Puchi-Cabrera, Hardness properties and high-temperature wear behaviour of nitrided AISI D2 tool steel, prior and after PAPVD coating, Wear 267 (2009) 1452–1461.

[37] W. Brostow, H.E. Hagg Lobland, Materials: Introduction and Applications, John Wiley & Sons, 2017.